Spatial Variability of SEBAL Estimated Root Zone Soil Moisture Across Scales

Sung-ho Hong†*, Kevin Lenth‡, Robert Aumer‡, Brian Borchers‡ and Jan M.H. Hendrickx§

†Department of Geosciences, Murray State University, Murray, KY, USA

‡Department of Mathematics, New Mexico Tech, Socorro, NM, USA

§Department of Earth and Environmental Science, New Mexico Tech, Socorro, NM, USA

*Corresponding Author

shong4@murraystate.edu Department of Geosciences, 310 Blackburn Hall, Murray State University, Murray, KY 42071, USA

Abstract

This study investigated the spatial scaling behavior of root zone soil moisture obtained from optical/thermal remote sensing observations. The data for this study were obtained from Landsat and Moderate Resolution Imaging Spectroradiometer (MODIS) satellites on five different dates between early spring (April) and fall (September) in the years from 2000 to 2004 in the semi-arid middle Rio Grande Valley of New Mexico. Soil moisture data were obtained using the Surface Energy Balance Algorithm for Land (SEBAL) algorithm. The data were spatially aggregated and checked for power law behavior over a range of scales from 30 m to 15 km for Landsat and from 1 km to 28 km for MODIS images. Results of this study demonstrate that power law scaling of soil moisture in the middle Rio Grande area holds up to 1 km^2 pixel size, but is no longer valid beyond that scale. While previous studies have studied soil moisture in the top 5 cm of the soil using radar and point measurements, our study uses SEBAL to estimate root-zone soil moisture. Our study is consistent with these previous studies in showing that variation in root-zone soil follows an empirical power law for pixel sizes of up to about 10^6 m^2 and that there is an apparent break in the scaling at larger scales.

1. Introduction

Information on the spatio-temporal distribution of soil moisture on regional scales can improve the quality of predictions by hydrological, meteorological and general circulation models, including processes such as evapotranspiration and runoff, precipitation, and atmospheric variability (Houser et al. 1998; van de Hurk et al. 1997; Entekhabi, Nakamura, and Njoku 1994; Hendrickx et al. 2016). However, soil moisture observations of larger regions are extremely difficult because soils vary from location to location as a result of soil forming processes that depend on geological parent material, topography, climate, plant and animal life, and time (Engle et al. 2010; Engle et al. 2014). As a result soil moisture exhibits a large spatial and temporal variability that has been documented in many studies. Since direct measurements on the ground are too expensive and time consuming for application on a watershed scale, only data from remote sensing can provide a cost-effective solution (Hendrickx et al. 2006; Ahmad and Bastiaanssen 2003; Rahimzadeh-Bajgiran et al. 2013; Bezerra et al. 2013; Fleming, Hendrickx, and Hong 2005). In this study, a remote sensing algorithm, Surface Energy Balance Algorithm for Land (SEBAL), was selected to estimate averaged soil moisture in the entire root zone. The root zone of most vegetation ranges from zero to about 500 cm (Canadell et al. 1996; Schenk and Jackson 2002) and soil water in the root zone supports transpiration via root extraction.

Few papers have examined sub-pixel variability in semi-arid regions and the effect of different up-scaling schemes on the relative accuracy of the aggregated data despite their practical importance; therefore, there is a need for more studies on the spatial

organization of soil moisture. The most complete studies on spatial correlation of environmental variables over different scales have dealt with ground measurements and remotely sensed radar observations of soil moisture in the top 0-5 cm of soils (Jackson, Schumgge, and Engman 1997; Jackson and O'Neill 1986). Rodriguez-Iturbe et al. (1995) analyzed Electronically Scanned Thinned Array Radiometer (ESTAR) microwave data and point measurements of soil moisture from the Washita '92 experiment. The variance of soil moisture was plotted on a log-log plot versus the pixel size for a range of pixel sizes from 10^3 m^2 (30 m by 30 m) to 10^8 m^2 (10 km by 10 km). They found that the variance of the soil moisture followed an empirical power law

$$\sigma_s^2 = c\, A^{\alpha} \tag{1}$$

or

$$\log_{10} \sigma_s^2 = c + \alpha \log_{10} A \tag{2}$$

where S is the relative degree of soil saturation (0-1), σ_s^2 is the variance of S, c is a constant, A is the pixel area and α is an exponent. They also confirmed that, as theory dictates, the spatial correlation fell off at larger distances according to a power law. Kim and Barros (2002) analyzed the ESTAR radiometer data from the Southern Great Plains (SGP) 1997 experiment. This dataset covered a much larger region than the earlier Washita '92 data set. They found that there was a break in the scaling of the soil moisture variance in this data set at a pixel size of about 10^8 m^2. For scales above and below this break, the variance followed a power law, but the exponents were different in the two scale ranges. Another analysis of the SGP '97 data using semi-variograms also found that there were two different scales of spatial correlation, with a break at roughly 30 km or almost 10^9 m^2 (Ryu and Famiglietti 2006).

The main goal of this study is to explore the spatial organization of soil moisture fields in a semi-arid environment, and especially to examine the power law behavior of the root zone soil moisture maps generated by the remote sensing algorithm SEBAL. This study is novel since previous multi-scaling studies on soil moisture dealt with soil moisture in the top 0-5 cm of the soil (Jackson, Schumgge, and Engman 1997; Jackson and O'Neill 1986) while our study deals with root zone soil moisture. Root zone soil moisture rather than surface soil moisture is often the critical parameter for weather prediction and global circulation models since it determines the partition of available energy at the earth's surface between latent and sensible heat fluxes (e.g. Akuraju et al. 2013; Seneviratne et al. 2010).

2. Methods and Materials

2.1 Study area

The study area covers an entire Landsat image (path 38, row 36) in semi-arid central New Mexico. It includes the middle Rio Grande Valley and the Estancia Basin as well as the Manzano and Sandia Mountain ranges (Figure 1). The area can generally be characterized by a narrow strip of about 2 km to 10 km of riparian and irrigated agricultural land on either side of the Rio Grande, mountain ranges with a width varying from about 5 km to 20 km, and highland deserts and rangelands covering the remaining area. The average annual air temperature is 15 °C. Daily summer temperatures range from 20 to 40 °C, while daily winter temperatures range from -12 to 10 °C. Mean annual precipitation is about 25 cm with more than half of the rainfall being monsoonal in summer and mean annual potential ET being approximately 150 cm.

2.2 Satellite Images

In this study, root zone soil moisture in degree of saturation at the time of satellite pass-over was estimated from five Landsat (30 m × 30 m resolution) and one Moderate Resolution Imaging Spectroradiometer (MODIS) (1000 m × 1000 m) image during 2000 to 2004 (Figure 1 and Table 1). For the date of 16 June 2002 both Landsat and MODIS images are available; therefore we estimated soil moisture also from the MODIS image to compare it and its scaling behavior to the Landsat estimates. The path and row of all the Landsat images used in this study are 33 and 36. Since the MODIS image covers a much bigger area (swath: 2,330 km), we took a subset of the MODIS image covering the same area as the Landsat image (Figure 1).

2.3 Surface Energy Balance Algorithm for Land (SEBAL)

SEBAL and its descendant METRIC (Mapping EvapoTranspiration at high Resolution with Internalized Calibration) are remote sensing flux algorithms that compute the surface energy balance on an instantaneous time scale for every pixel of a satellite image (Allen, Tasumi, and Trezza 2007; Bastiaanssen et al. 2005; Hendrickx and Hong 2005a). SEBAL and METRIC have demonstrated a high accuracy for evaporation mapping worldwide with typical accuracies of about ±15% and ±5% for, respectively, daily and seasonal evaporation estimates (Bastiaanssen et al. 2005; Hendrickx and Hong 2005a; Allen et al. 2007; Karimi and Bastiaanssen 2015; Hong 2008). The most innovative component of SEBAL and METRIC is their use of a near-surface temperature gradient which is indexed to satellite radiometric surface temperature. Thus, there is no need for absolute surface temperature calibration and air temperature measurements at each pixel for estimating the sensible heat flux at the surface. Both

models require an internal calibration for each image using inverse modelling at extreme conditions such as a “hot” or “dry” and “cold” or “wet” pixel to derive estimations of the sensible heat flux and to counteract systematic biases in net radiation, soil heat flux, radiometric temperatures and aerodynamic estimates (Allen, Tasumi, and Trezza 2006). METRIC differs from SEBAL in its use of high quality hourly weather data for calculation of the reference evapotranspiration that is used for evaluation of energy balance conditions at “cold” pixels where most incoming energy is used for evapotranspiration (Allen et al. 2011). For lack of high quality meteorological data we used SEBAL for this study; its use is justified because SEBAL estimates of evapotranspiration for the environmental conditions in the Middle Rio Grande Valley compared well with eddy covariance latent heat measurements (Hong 2008; Hendrickx and Hong 2005b). Detailed descriptions of SEBAL have been presented in the literature (Bastiaanssen et al. 1998; Allen, Tasumi, and Trezza 2007; Allen et al. 2011; Hong 2008).

SEBAL and METRIC are operational models for evapotranspiration mapping at high spatial resolution in areas covering a few hundred km in scale and are quite different from some more generally based remote sensing models for routine applications at the subcontinent scale such as the Atmosphere-Land-Exchange Inverse (ALEXI) (Anderson et al. 2007; Anderson et al. 2004). However, due to the required internal calibration of SEBAL and METRIC their implementation cannot be accomplished without trained experts with strong backgrounds in energy balance and radiation physics and familiarity with vegetation characteristics and agricultural practices (Allen et al. 2011). Under ideal conditions with full vegetation cover in irrigated areas without antecedent precipitation

the internal calibration is clear-cut. Those were the conditions encountered in this study so that the SEBAL implementations by the senior author were straightforward. But challenging conditions do occur and require a more creative internal calibration analysis or sometimes may prohibit the use of SEBAL and METRIC altogether. For example, several investigators (French et al. 2005a, 2005b; Long and Singh 2013; Tang et al. 2013; Timmermans et al. 2007; Long, Singh, and Li 2011) discuss how SEBAL and METRIC cannot be used when no wet and/or dry pixel exists in the image under consideration. However, co-author Hendrickx after analysis of hundreds of images in hot arid (e.g. Hendrickx et al. 2011; Hendrickx, Hearer, et al. 2005; Hendrickx and Hong 2005b; Compaoré et al. 2008) as well as humid tropical and temperate regions (e.g. Hendrickx, Bastiaanssen, et al. 2005; Wohl et al. 2012; Hendrickx et al. 2016) almost never encountered an image without a wet and/or dry pixel. Under arid conditions Landsat images have occasionally been encountered without any wet pixel but –even then– extension of the analysis to include the image above or below the image of interest in the same Landsat path will typically yield a reasonable extreme wet condition. Under humid conditions the main issue is cloudiness (e.g. Ju and Roy 2008; Sano et al. 2007) not finding a reasonable dry condition. Even where antecedent precipitation drives up the evaporation rate of the dry pixel, one often can estimate its sensible heat flux by using a simple soil water balance model (e.g. Allen 2011; Allen et al. 1998) and proceed with the internal calibration (Allen et al. 2011).

A more challenging issue is how pixel size affects the SEBAL estimated evapotranspiration rates (e.g. Tang et al. 2013). Finding a representative homogeneous wet or dry Landsat pixel of 30 m × 30 m in the reflectance bands or 60 × 60, 100 × 100

or 120 m × 120 m in, respectively, the thermal band of Landsat 7, 8 or 5 is straightforward under many environmental conditions, especially where relatively large irrigated fields are located in arid regions. However, finding a representative wet or dry pixel on a MODIS image with 1000 m × 1000 m pixels in the thermal band is quite challenging. Trezza, Allen, and Tasumi (2013) recommend using a cross-calibration between MODIS and Landsat applications of METRIC and successfully demonstrate their method using imagery of the Middle Rio Grande Valley. We have compared in-depth the outcome of SEBAL applications on 16 June 2002 on a Landsat and MODIS image and found good agreement between their SEBAL estimated ET maps (Hong, Hendrickx, and Borchers 2009, 2011). Therefore, we are confident that the 16 June 2002 soil moisture images of Landsat and MODIS have the quality needed for this study.

2.4 Evaporative Fraction Method for Root zone Soil Moisture Retrieval

The evaporative fraction (Λ) is defined as (Brutsaert and Sugita 1992; Crago 1996):

$$\Lambda = \frac{L}{L+H} \approx \frac{(\mathrm{ET})_\mathrm{a}}{(\mathrm{ET})_\mathrm{p}} \tag{3}$$

and can be calculated for each pixel using the output of SEBAL. Where L is the latent heat flux, H is the sensible heat flux, $(\mathrm{ET})_\mathrm{a}$ is the actual evapotranspiration and $(\mathrm{ET})_\mathrm{p}$ is the potential evapotranspiration. The relative degree of saturation in the root zone can be defined as the ratio of actual plant available water (W) over the soil water holding capacity (SWHC) or the ratio between the actual (θ) and saturated (θ_s) volumetric soil water contents in the root zone

$$S = \frac{W}{(\mathrm{SWHC})} \approx \frac{\theta}{\theta_\mathrm{s}} = f\left(\frac{L}{L+H}\right) = f(\Lambda). \tag{4}$$

The *Evaporative Fraction Method* for root zone soil moisture is based on the long-known soil physical relationship between the relative degree of saturation in the root zone (S) and the evaporative fraction (Λ) that quantifies the partitioning of sensible (H) and latent heat (L) fluxes at the land surface (e.g. Davies and Allen 1973; De Bruin 1983; Kustas and Norman 1999; Owe and van de Griend 1990; Budyko 1956; Manabe 1969; Thornthwaite 1948; Boni, Entekhabi, and Castelli 2001). Eq. [4] is also called the water stress function and can be either derived from physical principles (e.g. Campbell and Norman 1998) or modelled empirically using latent heat flux and soil moisture measurements (e.g. Scott, Bastiaanssen, and Ahmad 2003; Stewart and Verma 1992). Many different forms have been used to capture the stress function, ranging from linear (e.g. Mahfouf and Noilhan 1991), piecewise linear or threshold models (e.g. Deardorff 1977; Manabe 1969), to non-linear models (Anderson et al. 2007; Campbell and Norman 1998; Scott, Bastiaanssen, and Ahmad 2003). In addition, pixel size and sub-pixel soil moisture variability may also affect the optimal form (Chen et al. 1996). However, despite these differences the functions all look very similar (Figure 2). The non-linear function by Anderson et al. (2007) does not allow for much change in ET until the available water fraction becomes 0.6 while the one by Scott, Bastiaanssen, and Ahmad (2003) produces a steeper decrease of ET when the fraction falls below 0.2. In addition, these non-linear functions often require detailed soil information such as field capacity and wilting point that is not readily available. When soil information is uncertain some authors prefer linear forms for large scale applications so that evapotranspiration has a constant sensitivity to soil moisture conditions in the root zone (Betts et al. 1997; Song et al. 2000). Although the different expressions of Eq. [4] shown in Figure 2 appear to be empirical functions, they are based in fact on sound

science and have been successfully used for over sixty years by hydrologists and climatologists. The maximum difference between the three functions in Figure 2 is about 20% at the high and low ends of the evaporative fraction. Even though the absolute values derived for the relative degree of saturation in the root zone depend on the specific function used, because these functions are monotone increasing, the ranking of relative degrees from wet to dry will be similar and does not depend on the function used.

In this study we use an expression of Eq. [4] that is based on *in situ* root zone soil moisture measurements and validated evaporative fraction data from SEBAL (Ahmad and Bastiaanssen, 2003)

$$S = \mathrm{e}^{\frac{\Lambda-1}{0.42}} \cong \frac{W}{W_{\max}} \tag{5}$$

where S is degree of saturation, W is the actual plant available water and $W_{\max}$ is the maximum plant available water. The soil moisture measurements were obtained on grassland in Kansas on alluvial soils and loess (Smith et al. 1992) as well as in rainfed (vineyard, barley, wheat) and irrigated crops (maize, alfalfa) in Central Spain on sandy loams (Bastiaanssen et al. 1997; Bolle et al. 1993).

Validation and testing of Eq. [5] was conducted using soil moisture data from irrigated fields in Pakistan and Mexico. In Pakistan, volumetric soil water content was measured in alluvial soils with cotton and wheat at four depths with 25 cm intervals to a maximum depth of 100 cm. In Mexico, soil moisture was measured at depth 45 cm in vertisols on irrigated plots of wheat and alfalfa with the majority of active roots in the first 100 cm

below the surface. The comparison of Eq. [5] against these data yielded root mean square error of 0.05 cm^3cm^{-3}; and error was less than 0.07 cm^3cm^{-3} in 90% of cases (Scott et al., 2003). Based on the good performance of Eq. [5] under a wide range of environmental conditions some researchers have concluded that it is minimally affected by vegetation type or soil type and may have general applicability (Scott et al., 2003).

One *qualitative validation* was conducted in the swamps of the Upper Nile over an area of almost one million square kilometers using NOAA-AVHHR images (Mohamed, Bastiaanssen, and Savenije 2004). Another qualitative validation of Eq. [5] was conducted by co-author Hendrickx and his students (Fleming, Hendrickx, and Hong 2005). A SEBAL soil moisture map with a spatial resolution of 30 m × 30 m was generated from a Landsat 7 image of the Middle Rio Grande Basin for 16 June 2002. Soil moisture values were plotted along three transects perpendicular to the Rio Grande. Approximate land use and ground conditions were determined from the Landsat image and field observations in March 2005. The observed conditions in the field confirmed quite well the soil moisture conditions obtained from the satellite image. The high resolution of the approach was demonstrated in the sharp changes observed in association with roads, buildings, and vegetation changes along these heterogeneous transects (Fleming, Hendrickx, and Hong 2005).

The innovative elements of the evaporative fraction method are: (1) the derivation of soil moisture contents that are depth-averaged through the root zone of standing vegetation and with high spatial resolution (30 m × 30 m for Landsat to 250 m × 250 m to 1000 m × 1000 m MODIS) and broad coverage (for example, approximately 24,000

km^2 for a Landsat image); (2) multi-temporal coverage over vegetative or crop growth cycles; (3) the use of routinely available satellite images at no cost in the USA; and (4) relatively low costs of data processing. The method does have some interesting behavioral characteristics. The moisture that is evaporated and transpired originates in most cases throughout the entire vegetative root zone, typically one meter for many fully established irrigated crops (Allen et al., 1998b). However, the actual root zone depth at the time of retrieval will depend on the stage of vegetative or crop development and could be less than one meter. Mature forest systems may root much deeper and have rooting depths of several meters. Because there is no vegetation index specified as a baseline for Λ, the θ/θ_s predicted from Eq. [5] tends to increase with increase in vegetation mass and cover. Thus, as the vegetation index tends towards zero, θ/θ_s tends to represent the depth of the evaporative layer of soil (0-10 or 15 cm), which serves as the source depth for direct evaporation. As the vegetation index tends towards values representing full vegetation and soil cover, θ/θ_s tends toward representing the full depth of the effective rooting zone. Therefore, this method is optimal for the investigation of the available water storage in soils. It stands clearly apart from active and passive radar satellites that measure soil moisture to approximately constant penetration depths of a few cm (e.g. Miller, Hendrickx, and Borchers 2004; Wickel, Jackson, and Wood 2001; Hendrickx, Rabus, et al. 2009; Romero-Suarez 2010; McNairn, Pultz, and Boisvert 2002; Jackson 2002). A limitation of soil moisture retrievals, using the evaporative fraction as derived from SEBAL or METRIC using optical and thermal imagery, is that the method can only be employed on clear days without clouds while radar systems operate under all weather conditions. However, soil surface evaporation process models or distributed hydrologic models (Downer and Ogden 2003; Downer and Ogden 2004;

Hendrickx, Pradhan, et al. 2009; Daniel B. Stephens & Associates 2010) can be operated in between satellite overpass dates to create continuous soil water records that are calibrated and targeted to the satellite retrievals (Hendrickx et al. 2016).

3. Data description and procedure

Once soil moisture maps were generated from SEBAL, 30 m × 30 m resolution of Landsat- and 1000 m × 1000 m of MODIS- based soil moisture data were aggregated to 15,000 m and 28,000 m resolutions, respectively. Aggregation imagery was obtained by calculating the arithmetic mean over an $n \times n$ window. If any pixel in an $n \times n$ window was outside of the data set, the entire window was excluded. For the semi-variogram model, computing experimental semi-variograms using every pixel at the 30 m × 30 m scale proved infeasible, since the images used in this study were very large; instead, a random sampling strategy was used. Ten 2,500 pixel samples were randomly selected from the soil moisture image and experimental semi-variograms were calculated for each sample. These ten experimental semi-variograms were then averaged together.

4. Spatial distribution and scaling behavior of root zone soil moisture

Figure 1 presents the soil moisture map of the Landsat 5 image on 16 June 2002 as an example produced by SEBAL. Higher soil moisture is observed in the riparian areas and mountain forests while low to very low soil moisture occurs in the surrounding deserts. The city of Albuquerque has somewhat higher soil moisture than the surrounding desert areas due to grass and trees in the urban environment.

Table 1 shows temporal changes in soil moisture; it increases from 7 April (mean: 0.11), just after the start of the growing season, to 31 July (mean: 0.21) at the height of the growing as well as monsoon season. Then a decrease of soil moisture is observed on 14 September (mean: 0.09) after the monsoon. Higher standard deviations are found in the images of June and July; that is due to the fact that the difference in soil moisture between riparian and mountain (high soil moisture) and desert and bare soils (low soil moisture) is greater during the summer monsoon growing season. The mean value of the soil moisture on 7 April (0.11) is greater than that of 9 May (0.06) (Table 1). This reflects some soil moisture accumulation during the winter period before 7 April when vegetation is dormant as well as the lack of precipitation between 1 April and 9 May when the vegetation starts transpiring at the start of the growing season.

For the 16 June image, the disparate spatial resolutions of Landsat- and MODIS-based soil moisture images result in differences in soil moisture distribution (Figure 1). Many small areas (length scale on the order of 10 to 100 m) with high soil moisture along the river are captured well in the Landsat-based soil moisture map with a spatial resolution of 30 m; however, these peak soil moistures are averaged out in the MODIS-derived soil moisture map with a spatial resolution of 1000 m. Besides the difference in the spatial resolution, a difference in radiance measurements between the Landsat and MODIS and different satellite overpass times (the Landsat overpass time was 10:30 am Mountain Standard Time (MST) while the MODIS time was 11:00 am MST) also results in slightly different soil moisture estimates (Figure 1 and Table 1). However, the overall spatial distribution of soil moisture maps and basic statistics reveal that the

SEBAL algorithm produced very similar soil moisture estimates from either Landsat or MODIS imagery.

In order to examine the power law behavior of soil moisture maps, soil moisture variances for different pixel sizes were calculated (Figure 3). In all cases except 7 April, log variances decrease and display a fairly linear trend until the pixel size reaches about 10^6 m^2, approximately a 1 km length scale. Furthermore, although the intercept varies with the overall moisture, the slope of each curve (the exponent alpha in the power law) is similar. Some of the values of variance after 10^8 m^2 pixel size waggle because there are few data points. Also, the log variances of the April image linearly decrease until 10^8 m^2 and the slope is steeper after 10^8 m^2 pixel size. This is similar to the results of Ryu and Famiglietti (2006) who also reported a non-linear trend in their data. They concluded that smaller scale correlation (10 km to 30 km pixel length) is caused by land surface features like vegetation and soil texture, while larger scale correlation (60 km to 100 km) is caused by regional precipitation. Changes in variances with pixel size between Landsat and MODIS-based soil moisture on 16 June 2002, follow a similar trend.

Also note that the log variances of each starting point (30 m × 30 m pixel size) for all five dates are different from each other but the slope of the variances with pixel size are all similar except for the April imagery. The 7 April image is the only image prior to the growing season, when vegetation is not transpiring and thus the soil moisture conditions of the top 10 to 20 cm are captured by the SEBAL estimated root zone soil moisture algorithms. Therefore, the effect of vegetation is minimal in this image while the effect

of precipitation on spatial variability of soil moisture dominates. This observation is supported by the larger correlation length in the semi-variogram of 7 April (Figure 4) and is similar to the result of Rye and Famiglietti (2006) discussed above.

In order to examine the anisotropic variance, semi-variograms were calculated in four compass directions; N-S, E-W, NE-SW and NW-SE. There were no significant differences within the four directional experimental semi-variograms, and thus we assume an isotropic semi-variogram. The sampling technique was then repeated to produce an omni-directional experimental semi-variogram (Figure 4). In the semi-variograms, sill (gamma) values are dependent upon the variance of the soil moisture maps. In addition to sill, the range of each semi-variogram also changes with the soil moisture conditions. Soil moisture maps during the summer have higher mean and standard deviation and have ranges around 30 km, but low soil moisture conditions (May and September) have ranges around 10 km. Smaller ranges during a low soil moisture condition are revealed from the spatial distribution of soil moisture; high soil moisture is found only along the narrow strip of Rio Grande riparian areas and in mountain forests with lateral scales up to about 10 km while the surrounding areas are very dry. Although the sill of the Landsat semi-variogram on 16 June 2002 is slightly higher than MODIS semi-variogram, both semi-variograms have a similar shape. This is another validation that the SEBAL algorithm produces very similar soil moisture estimates from Landsat and MODIS images. The lower sill of the MODIS semi-variogram is expected since MODIS pixels are about one order of magnitude larger than Landsat pixels which will temper extreme soil moisture values.

5. Conclusions

The main goal of this study was to examine the power law behavior of SEBAL estimated root zone soil moisture from Landsat and MODIS imagery. In most cases, the slope of changes in variances with pixel size are similar, and power law scaling of soil moisture holds up to 10^6 m^2 pixel size; a power law fit is no longer valid beyond that scale. Semi-variograms show an isotropic correlation structure and their sill and range are dependent upon the root zone soil moisture conditions. Results of this study also verify that the SEBAL algorithm produces very similar soil moisture maps from Landsat and MODIS images.

Previous studies have studied soil moisture in the top 5 cm of the soil using radar and point measurements while our study uses SEBAL/METRIC to estimate root-zone soil moisture. Our study is consistent with previous studies in showing that variation in root-zone soil follows an empirical power law for pixel sizes of up to about 10^6 m^2 and that there is an apparent break in the scaling at larger scales.

Acknowledgements

This study was funded by the Army Research Office, STIR grant: W911NF-09-1-0006.

References

Ahmad, M.D., and W. Bastiaanssen. 2003. "Retrieving soil moisture storage in the unsaturated zone using satellite imagery and bi-annual phreatic surface fluctuations." *Irrigation and Drainage Systems* 17:141-61.

Akuraju, V.R., D. Ryu, B. George, Y. Ryu, and K. Dassanayake. 2013. "Analysis of root-zone soil moisture control on evapotranspiration in two agriculture fields in Australia." *20th International Congress on Modelling and Simulation*:3064-70.

Allen, R. G., L. S. Pereira, D. Raes, and M. Smith. 1998. *Crop evapotranspiration: Guidelines for computing crop requirements. Irrigation and Drainage Paper No. 56.* Vol. 56, *FAO Irrigation and drainage paper*. Rome, Italy: Food and Agricultural Organization of the United Nations.

Allen, R.G., M. Tasumi, A. Morse, R. Trezza, J.L. Wright, W. Bastiaanssen, W. Kramber, I. Lorite, and C.W. Robison. 2007. "Satellite-based Energy Balance for Mapping Evapotranspiration with Internalized Calibration (METRIC) – Applications." *Journal of Irrigation and Drainage Engineering* 133:395-406.

Allen, R.G., M. Tasumi, and R. Trezza. 2006. "Benefits from tying satellite-based energy balance to reference evapotranspiration " In *Earth Observation for Vegetation Monitoring and Water Management*, edited by G. D'Urso, A. Jochum and J.Moreno, 127-37. Naples, Italy: American Institute of Physics.

———. 2007. "Satellite-based Energy Balance for Mapping Evapotranspiration with Internalized Calibration (METRIC) – Model." *Journal of Irrigation and Drainage Engineering* 133:380-94.

Allen, Richard G. 2011. "Skin layer evaporation to account for small precipitation events—An enhancement to the FAO-56 evaporation model." *Agricultural Water Management* 99 (1):8-18. doi: http://dx.doi.org/10.1016/j.agwat.2011.08.008.

Allen, Richard G., Ayse Irmak, Ricardo Trezza, Jan M.H. Hendrickx, Wim G.M. Bastiaanssen, and Jeppe Kjaersgaard. 2011. "Satellite-based ET estimation in agriculture using SEBAL and METRIC." *Hydrologic Processes* 25:4011–27.

Anderson, M. C., J. M. Normal, W. P. Kustas, F. Li, J. H. Prueger, and J. R. Mecikalski. 2007. "A climatological study of evapotranspiration and moisture stress across the continental United States: 1. Model formulation." *J. Geophys. Res.* 112:D11112, doi:10.1029/2006JD007507.

Anderson, M.C., J.M. Norman, J.R. Mecikalski, R.D. Torn, W.P. Kustas, and J.B. Basara. 2004. "A multi-scale remote sensing model for disaggregating regional fluxes to micrometeorological scales." *J. Hydrometeor.* 5:343-63.

Bastiaanssen, W. G. M., H. Pelgrum, P. Droogers, H.A.R. de Bruin, and M. Menenti. 1997. "Area-averaged estimates of evaporation, wetness indicators and top soil moisture during two golden days in EFEDA." *Agric. For. Meteorol.* 87 (2-3):119-37.

Bastiaanssen, W.G.M., M. Menenti, R.A. Feddes, and A.A. M. Holtslag. 1998. "A remote sensing surface energy balance algorithm for land (SEBAL). Part 1: Formulation." *Journal of Hydrology* 212-213:198-212.

Bastiaanssen, W.G.M., E.J.M. Noordman, H. Pelgrum, G. Davids, B.P. Thoreson, and R.G. Allen. 2005. "SEBAL model with remotely sensed data to improve water-

resources management under actual field conditions." *Journal of Irrigation and Drainage Engineering* 131:85-93.

Betts, Alan K., Fei Chen, Kenneth E. Mitchell, and Zaviša I. Janjić. 1997. "Assessment of the Land Surface and Boundary Layer Models in Two Operational Versions of the NCEP Eta Model Using FIFE Data." *Monthly Weather Review* 125 (11):2896-916. doi: 10.1175/1520-0493(1997)125<2896:aotlsa>2.0.co;2.

Bezerra, B., C Santos, B Silva, A Perez-Marin, M Bezerra, J Bezerra, and T Rao. 2013. "Estimation of soil moisture in the root-zone from remote sensing data." *Revista Brasileira de Ciência do Solo* 37:596-603.

Bolle, H.-J., J.-C. André, J.L. Arrue, H.K. Barth, P. Bessemoulin, A. Brasa, H.A.R. de Bruin, et al. 1993. "EFEDA: European field experiment in a desertification-threatened area." *Ann. Geophys.* 11:173-89.

Boni, Giorgio, Dara Entekhabi, and Fabio Castelli. 2001. "Land data assimilation with satellite measurements for the estimation of surface energy balance components and surface control on evaporation." *Water Res. Res.* 37 (6):1713-22

Brutsaert, W. , and M. Sugita. 1992. "Application of self-preservation in the diurnal evolution of the surface energy budget to determine daily evaporation." *J. of Geophysical Res.* 97 (D17):18377-82.

Budyko, M.I. 1956. *Heat balance of the earth's surface (in Russian)*. Leningrad, USSR: Gidrometeoizdat.

Campbell, G.S. , and J.M. Norman. 1998. *An introduction to environmental biophysics. Second Edition*. New York, NY: Springer.

Canadell, J., R. B. Jackson, J. B. Ehleringer, H. A. Mooney, O. E. Sala, and E. D. Schulze. 1996. "Maximum rooting depth of vegetation types at the global scale." *Oecologia* 108 (4):583-95.

Chen, F., K. E. Mitchell, John Schaake, Yongkang Xue, Hua-Lu Pan, Victor Koren, Qing Yun Duan, Michael Ek, and Alan Betts. 1996. "Modeling of land-surface evaporation by four schemes and comparison with FIFE observations." *Journal of Geophysical Research* 101:7251-68.

Compaoré, Halidou, Jan M. H. Hendrickx, Sung-ho Hong, Jan Friesen, Nick C. van de Giesen, Charles Rodgers, Joerg Szarzynski, and Paul L. G. Vlek. 2008. "Evaporation mapping at two scales using optical imagery in the White Volta Basin, Upper East Ghana " *Physics and Chemistry of the Earth, Parts A/B/C* 33:127-40, doi:10.1016/j.pce.2007.04.021.

Crago, R.D. 1996. "Comparison of the evaporative fraction and the Priestley-Taylor α for parameterizing daytime evaporation." *Water Resources Research* 32:1403-9.

Daniel B. Stephens & Associates, Inc. 2010. "Draft - Manual for the Distributed Parameter Watershed Model (DPWM)." In, 83. Albuquerque: Daniel B. Stephens & Associates, Inc.

Davies, J.A., and C.D. Allen. 1973. "Equilibrium, potential and actual evapotranspiration from cropped surfaces in southern Ontario." *J. Appl. Meteorol.* 12:649-57.

De Bruin, H.A.R. 1983. "A model for the Priestley-Taylor parameter alpha." *J. Clim. Appl. Meteorol.* 22:572-8.

Deardorff, J. W. 1977. "A Parameterization of Ground-Surface Moisture Content for Use in Atmospheric Prediction Models." *Journal of Applied Meteorology* 16 (11):1182-5. doi: 10.1175/1520-0450(1977)016<1182:apogsm>2.0.co;2.

Downer, C.W., and F. L. Ogden. 2003. "Prediction of runoff and soil moistures at the watershed scale: effects of model complexity and parameter assignment." *Water Res. Res.* 39 (3):1045, doi:10.29/2002WR001439.

Downer, C.W., and F.L. Ogden. 2004. "GSSHA: A model for simulating diverse streamflow generating processes." *J. Hydrol. Engrg.* 9:161-74.

Engle, E.M. , J.B.J. Harrison, J.M.H. Hendrickx, and B. Borchers. 2010. "Chapter 11. Digital soil boundary detection using quantitative hydrologic remote sensing." In *Digital Soil Mapping: Bridging Research, Environmental Application, and Operation*, edited by Janis L. Boettinger, David W. Howell, Amanda C. Moore, Alfred E. Hartemink and Suzann Kienast-Brown, 123-34. Dordrecht: Springer

Engle, E.M., J. Bruce J. Harrison, Jan M.H. Hendrickx, and Brian Borchers. 2014. "Remote sensing for soil map unit boundary detection." In *Military Geosciences in the 21st Century. Reviews in Engineering Geology Series*, edited by R.S. Harmon and E.V. MacDonald, 119-30. Geological Society of America.

Entekhabi, D., H. Nakamura, and E.G. Njoku. 1994. "Solving the inverse problems for soil-moisture and temperature profiles by sequential assimilation of multifrequency remotely-sensed observations." *IEEE Transactions on Geoscience and Remote Sensing* 32:438 - 48.

Fleming, K. , Jan M.H. Hendrickx, and Sung-ho Hong. 2005. "Regional mapping of root zone soil moisture using optical satellite imagery." *Proc. International Society for Optical Engineering, SPIE* 5811:159-70.

French, A. N., F. Jacob, M. C. Anderson, W. P. Kustas, W. Timmermans, A. Gieske, Z. Su, et al. 2005a. "Corrigendum to "Surface energy fluxes with the Advanced Spaceborne Thermal Emission and Reflection radiometer (ASTER) at the Iowa 2002 SMACEX site (USA)"." *Remote Sensing of Environment Remote Sensing of Environment* 99 (4):471.

———. 2005b. "Surface energy fluxes with the Advanced Spaceborne Thermal Emission and Reflection radiometer (ASTER) at the Iowa 2002 SMACEX site (USA)." *Remote Sensing of Environment Remote Sensing of Environment* 99 (1-2):55-65.

Hendrickx, J.M.H., W.G.M. Bastiaanssen, E.J.M. Noordman, Sung-ho Hong, and L.E. Calvo Gobbeti. 2005. "Estimation of regional actual evapotranspiration in the Panama Canal watershed." In *The Rio Chagres: A multidisciplinary profile of a tropical watershed*, edited by R.S. Harmon, 315-24. Dordrecht, The Netherlands: Springer.

Hendrickx, J.M.H., D.M. Hearer, Sung-ho Hong, B Borchers, and P Neville. 2005. "Land cover and evapotranspiration in the Middle Rio Grande Basin." *Eos Trans. AGU,* 86(52):Fall Meet. Suppl., Abstract H44B-05.

Hendrickx, J.M.H., and S.-H. Hong. 2005a. "Mapping sensible and latent heat fluxes in arid areas using optical imagery." *Proceedings of International Society for Optical Engineering, SPIE* 5811:138-46.

Hendrickx, J.M.H., S.-H. Hong, J. Friesen, H. Compaore, N.C. van de Giesen, C. Rodgers, and P.L.G. Vlek. 2006. "Mapping energy balance fluxes and root zone soil moisture in the White Volta Basin using optical imagery." *Proceedings of International Society for Optical Engineering, SPIE* 6239:238-49.

Hendrickx, Jan M.H. , Richard G. Allen, Al Brower, Aaron R. Byrd, Sung-ho Hong, Fred L. Ogden, Nawa Raj Pradhan, et al. 2016. "Benchmarking optical/thermal satellite imagery for estimating evapotranspiration and soil moisture in decision support tools " *Journal American Water Resources Association* 52 (1):89-119.

Hendrickx, Jan M.H., J. Bruce J. Harrison, Brian Borchers, Julie R. Kelley, Stacy Howington, and Jerry Ballard. 2011. "High-resolution soil moisture mapping in Afghanistan." *Proc. International Society for Optical Engineering, SPIE* 8017:801710; doi:10.1117/12.87255.

Hendrickx, Jan M.H., and Sung-ho Hong. 2005b. "Mapping sensible and latent heat fluxes in arid areas using optical imagery." *Proc. International Society for Optical Engineering, SPIE* 5811:138-46.

Hendrickx, Jan M.H., Nawa R. Pradhan, Sung-ho Hong, Fred L. Ogden, Aaron R. Byrd, and David Toll. 2009. "Improvement of hydrologic model soil moisture predictions using SEBAL evapotranspiration estimates." *Proc. International Society for Optical Engineering, SPIE* 7303:730311.

Hendrickx, Jan M.H., Bernhard Rabus, Diana C. Romero, Hans Wehn, J. Bruce J. Harrison, Sung-ho Hong, Brian Borchers, and Jim Slater. 2009. "Preliminary validation of Radarsat2 surface soil moisture estimates." *Proc. International Society for Optical Engineering, SPIE* 7303:730310.

Hong, Sung-Ho. 2008. "Mapping regional distributions of energy balance components using optical remotely sensed imagery." Ph.D. Dissertation, New Mexico Institute of Mining and Technology.

Hong, Sung-ho, Jan M. H. Hendrickx, and Brian Borchers. 2009. "Up-scaling of SEBAL derived evapotranspiration maps from Landsat (30 m) to MODIS

(250 m) scale." *Journal of Hydrology* 370:122-38; doi:10.1016/j.jhydrol.2009.03.002

———. 2011. "Down-scaling of SEBAL derived evapotranspiration maps from MODIS (250 m) to Landsat (30 m) scales." *International Journal of Remote Sensing* 32 (21):6457-77.

Houser, P.R., W.J. Shuttleworth, J.S. Famiglietti, H.V. Gupta, K.H. Syed, and D.C. Goodrich. 1998. "Integration of soil moisture remote sensing and hydrological modeling using data assimilation." *Water Resources Research* 34:3405-20.

Jackson, T.J. . 2002. "Passive microwave remote sensing methods." In *Methods of soil analysis. Part 4. Physical Methods*, edited by J.H. Dane and G.C. Topp, 488-97. Madison, Wisconsin: Soil Science Society of America.

Jackson, T.J. , and P.E. O'Neill. 1986. "Temporal observations of surface soil moisture using a passive microwave sensor." *IEEE Transactions on Geoscience and Remote Sensing* 21:281-96.

Jackson, T.J., T.J. Schumgge, and E.T. Engman. 1997. "Remote sensing applications to hydrology: soil moisture." *Hydrological Sciences Journal* 41:517-30.

Ju, Junchang, and David P. Roy. 2008. "The availability of cloud-free Landsat ETM+ data over the conterminous United States and globally." *Remote Sensing of Environment* 112 (3):1196-211. doi: http://dx.doi.org/10.1016/j.rse.2007.08.011.

Karimi, P., and W. G. M. Bastiaanssen. 2015. "Spatial evapotranspiration, rainfall and land use data in water accounting – Part 1: Review of the accuracy of the remote sensing data." *Hydrol. Earth Syst. Sci.* 19:507-32.

Kim, G. , and A. P. Barros. 2002. "Space-time characterization of soil moisture from passive microwave remotely sensed imagery and ancillary data." *Remote Sens. Environ.* 81:393- 403.

Kustas, W. P., and J.M. Norman. 1999. "Evaluation of soil and vegetation heat flux predictions using a simple two-source model with radiometric temperatures for partial canopy cover." *Agric. For. Meteorol.* 94:13-29.

Long, Di, and Vijay P. Singh. 2013. "Assessing the impact of end-member selection on the accuracy of satellite-based spatial variability models for actual evapotranspiration estimation." *Water Resources Research* 49 (5):2601-18. doi: 10.1002/wrcr.20208.

Long, Di, Vijay P. Singh, and Zhao-Liang Li. 2011. "How sensitive is SEBAL to changes in input variables, domain size and satellite sensor?" *Journal of Geophysical Research: Atmospheres* 116 (D21):n/a-n/a. doi: 10.1029/2011jd016542.

Mahfouf, J. F., and J. Noilhan. 1991. "Comparative Study of Various Formulations of Evaporations from Bare Soil Using In Situ Data." *Journal of Applied Meteorology* 30 (9):1354-65. doi: 10.1175/1520-0450(1991)030<1354:csovfo>2.0.co;2.

Manabe, Syukuro. 1969. "1. The atmospheric circulation and the hydrology of the earth's surface." *Monthly Weather Review* 97 (11):739-74.

McNairn, H., T.J. Pultz, and J.B. Boisvert. 2002. "Active microwave remote sensing methods." In *Methods of soil analysis. Part 4. Physical Methods*, edited by J.H. Dane and G.C. Topp, 475-88. Madison, Wisconsin: Soil Science Society of America.

Miller, T. W., J. M. H. Hendrickx, and B. Borchers. 2004. "Radar detection of buried landmines in field soils." *Vadose Zone J* 3:1116-27.

Mohamed, Y.A. , W.G.M. Bastiaanssen, and H.H.G. Savenije. 2004. "Spatial variability of evaporation and moisture storage in the swamps of the upper Nile studied by remote sensing techniques." *Journal of Hydrology* 289:145-64 doi:10.1016/j.jhydrol.2003.11.038.

Owe, M., and A.A. van de Griend. 1990. "Daily surface moisture model for large area semi-arid land applications with limited climate data." *Journal of Hydrology* 121:119-32.

Rahimzadeh-Bajgiran, P, A Berg, C Champagne, and K Omasa. 2013. "Estimation of soil moisture using optical/thermal infrared remote sensing in the Canadian Prairies." *Journal of Photogrammetry and Remote Sensing* 83:94-103.

Rodriguez-Iturbe, G. K. Vogel, R. Rigon, D. Entekhabi, F. Castelli, and A. Rinaldo. 1995. "On the spatial organization of soil moisture fields." *Geophys. Res. Lett.* 22 (20):2757- 60.

Romero-Suarez, Diana C. 2010. "Validation of Radarsat2 surface soil moisture measurements." M.S. Thesis, New Mexico Tech.

Ryu, D., and J.S. Famiglietti. 2006. "Multi-scale Spatial Correlation and Scaling Behavior of Surface Soil Moisture." *Geophysical Research Letters* 33:L.08404.

Sano, E. E., L. G. Ferreira, G. P. Asner, and E. T. Steinke. 2007. "Spatial and temporal probabilities of obtaining cloud-free Landsat images over the Brazilian tropical savanna." *International Journal of Remote Sensing* 28 (12):2739-52.

Schenk, H. Jochen, and Robert B. Jackson. 2002. "Rooting depths, lateral root spreads and below-ground/above-ground allometries of plants in water-limited ecosystems." *Journal of Ecology* 90 (3):480-94. doi: 10.1046/j.1365-2745.2002.00682.x.

Scott, Christopher A. , Wim G. M. Bastiaanssen, and Mobin-ud-Din Ahmad. 2003. "Mapping Root Zone Soil Moisture Using Remotely Sensed Optical Imagery." *J. Irrig. and Drain. Engrg.* 129 (5):326-35.

Seneviratne, Sonia I., Thierry Corti, Edouard L. Davin, Martin Hirschi, Eric B. Jaeger, Irene Lehner, Boris Orlowsky, and Adriaan J. Teuling. 2010. "Investigating soil moisture-climate interactions in a changing climate: A review." *Earth-Science Reviews* 99 (3/4):125-61.

Smith, E.A., A.Y. Hsu, W.L. Crosson, R.T. Field, L.J. Fritschen, R.J. Gurney, E.T. Kanemasu, et al. 1992. "Area-averaged surface fluxes and their time-space variability over the FIFE experimental domain." *J. of Geophysical Res.* 97 (D17):18599-622.

Song, J., M. L. Wesely, R. L. Coulter, and E. A. Brandes. 2000. "Estimating Watershed Evapotranspiration with PASS. Part I: Inferring Root-Zone Moisture Conditions Using Satellite Data." *Journal of Hydrometeorology* 1 (5):447-61. doi: 10.1175/1525-7541(2000)001<0447:ewewpp>2.0.co;2.

Stewart, J. B., and S. B. Verma. 1992. "Comparison of surface fluxes and conductances at two contrasting sites within the FIFE area." *Journal of Geophysical Research: Atmospheres* 97 (D17):18623-8. doi: 10.1029/92jd00256.

Tang, Ronglin, Zhao-Liang Li, Kun-Shan Chen, Yuanyuan Jia, Chuanrong Li, and Xiaomin Sun. 2013. "Spatial-scale effect on the SEBAL model for

evapotranspiration estimation using remote sensing data." *Agricultural and Forest Meteorology* 174–175:28-42. doi: http://dx.doi.org/10.1016/j.agrformet.2013.01.008.

Thornthwaite, C. 1948. "An approach towards a rational classification of climate." *Geographical Review* 38:55-94.

Timmermans, Wim J. , William P. Kustas, Martha C. Anderson, and Andrew N. French. 2007. "An intercomparison of the Surface Energy Balance Algorithm for Land (SEBAL) and the Two-Source Energy Balance (TSEB) modeling schemes." *Remote Sensing of Environment* 108:369-84.

Trezza, Ricardo, Richard Allen, and Masahiro Tasumi. 2013. "Estimation of Actual Evapotranspiration along the Middle Rio Grande of New Mexico Using MODIS and Landsat Imagery with the METRIC Model." *Remote Sensing* 5 (10):5397.

van de Hurk, B.J.J.M., W.G.M. Bastiaanssen, H. Pelgrum, and E. van Meijgaard. 1997. "A new methodology for assimilation of initial soil moisture fields in weather prediction models using Meteosat and NOAA data." *Journal of Applied Meteorology*, 36:1271-83.

Wickel, A. J., T. J. Jackson, and E. F. Wood. 2001. "Multitemporal monitoring of soil moisture with RADARSAT SAR during the 1997 Southern Great Plains hydrology experiment." *Int. J. Remote Sensing* 22 (8):1571-83.

Wohl, Ellen, Ana Barros, Nathaniel Brunsell, Nick A. Chappell, Michael Coe, Thomas Giambelluca, Steven Goldsmith, et al. 2012. "The hydrology of the humid tropics." *Nature Clim. Change* 2:655–62, doi:10.1038/nclimate556.

Table 1. Data used in this study. Rainfall data were obtained from the New Mexico Climate Center (http://weather.nmsu.edu/data/data.htm) and mean and standard deviation (STD) are estimated from Landsat (30 m x 30 m) and MODIS (1000 m x 1000 m) images.

Date	Satellite	Time since rain (days)			Root-zone soil moisture (unitless)	
		ACD[1]	BSE[2]	ATA[3]	Mean	SD*
7 April 2000	Landsat7	6	16	6	0.11	0.10
9 May 2000	Landsat7	30+	30+	30+	0.06	0.09
16 June 2002	Landsat7	1	20	3	0.15	0.13
16 June 2002	MODIS	1	20	3	0.15	0.11
31 July 2004	Landsat5	3	5	4	0.21	0.15
14 September 2000	Landsat7	5	16	14	0.09	0.10

[1]Alcalde ASC weather station, [2]Bosque RAWS weather station, [3]Artesia ASC weather station, *standard deviation

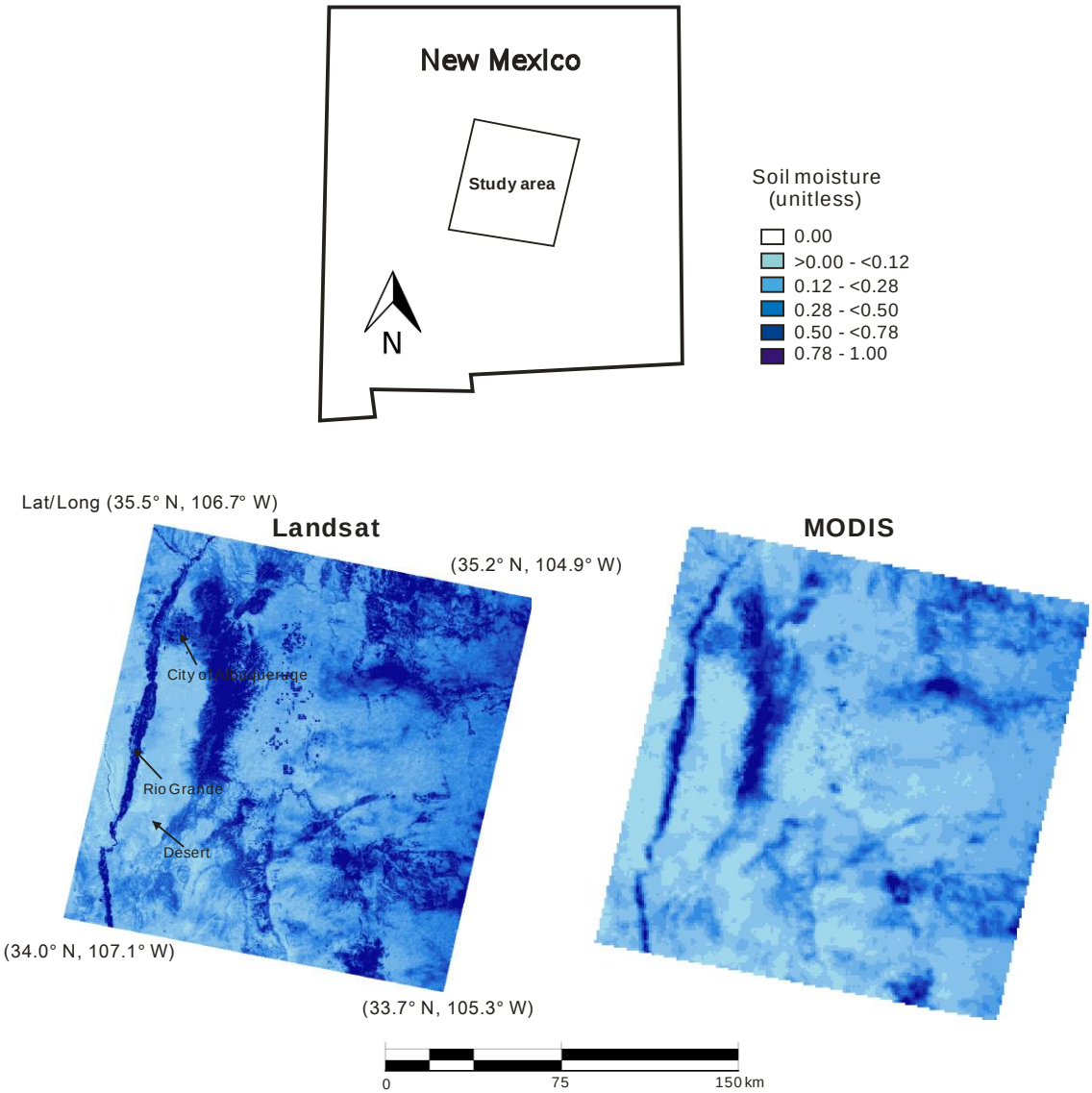

Figure 1. Study area and root zone soil moisture maps on 16 June 2002.

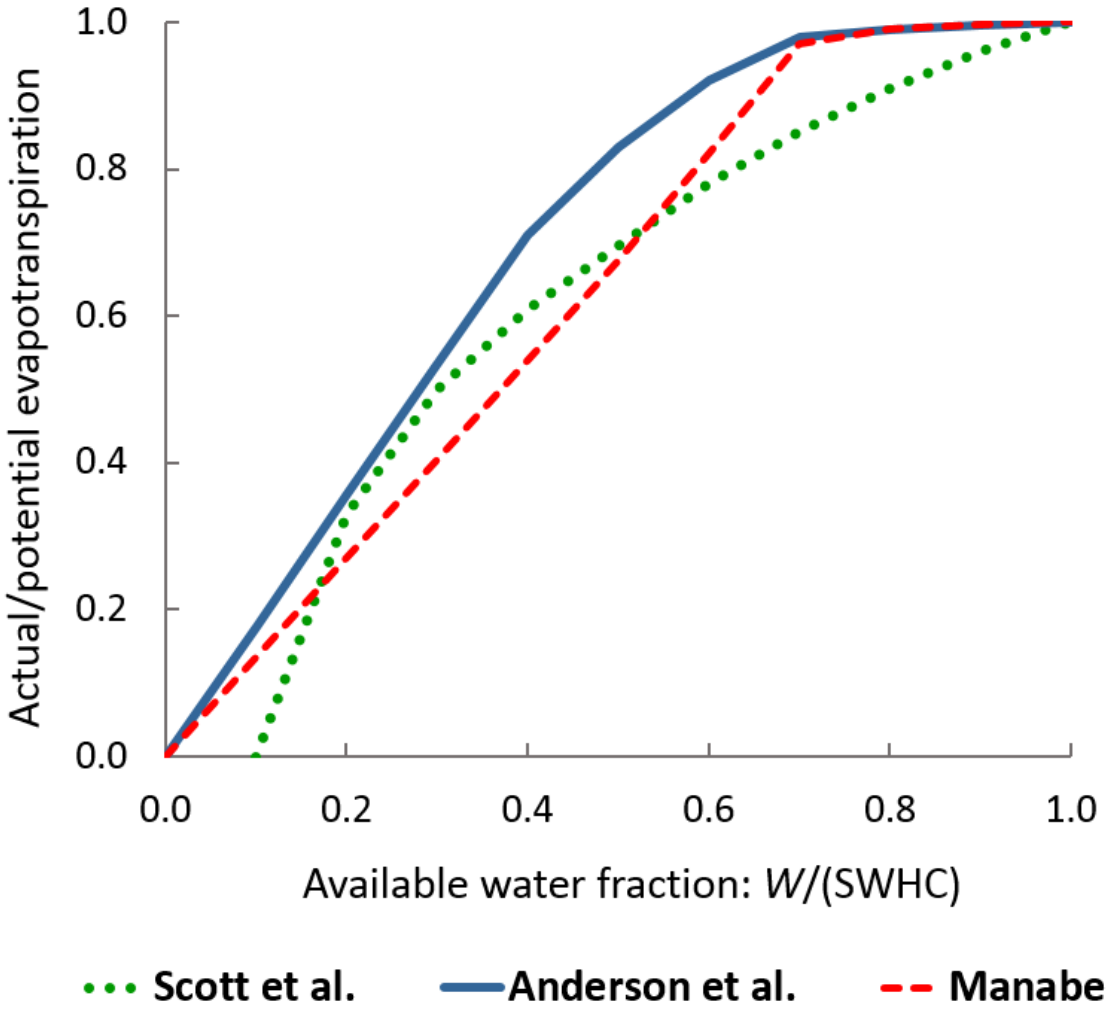

Figure 2. Non-linear and linear forms of the relationship between relative evapotranspiration (actual/potential evapotranspiration) and available water fraction (Anderson et al. 2007; Manabe 1969; Scott, Bastiaanssen, and Ahmad 2003).

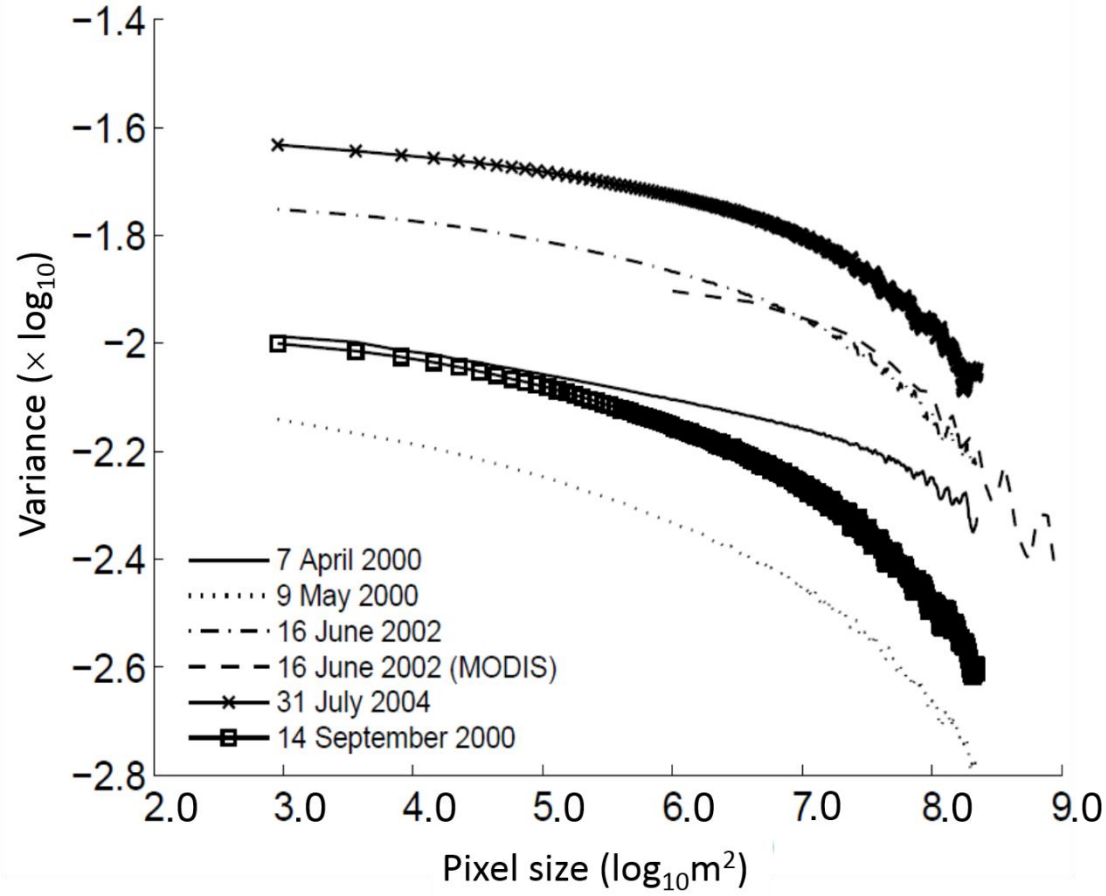

Figure 3. Change in soil moisture variance with pixel size.

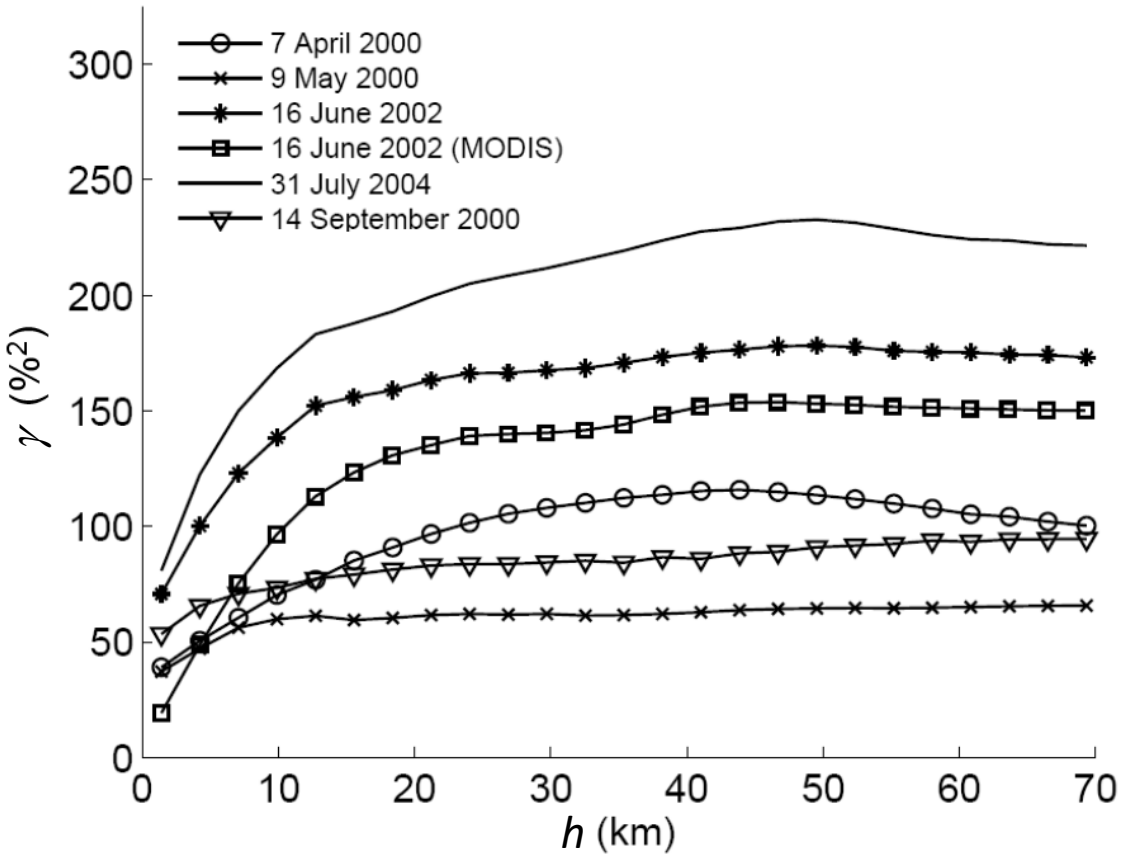

Figure 4. Semi-variogram of root zone soil moisture derived by SEBAL from Landsat and MODIS images, where *h* is the distance between pairs of points. Since root zone soil moisture is given as an unitless percentage, the semivariance (γ) is in units of $\%^2$.